Composites Science and Technology 135 (2016) 123–127

Contents lists available at ScienceDirect

Composites Science and Technology

journal homepage: http://www.elsevier.com/locate/compscitech

Strengthening and toughening effects by strapping carbon nanotube cross-links with polymer molecules

Jingyun Zou [a, b], Xiaohua Zhang [b, *], Jingna Zhao [b], Chaoshuai Lei [b], Yonghao Zhao [a], Yuntian Zhu [a, c], Qingwen Li [b, **]

[a] Nano Structural Materials Center, School of Materials Science and Engineering, Nanjing University of Science and Technology, Xiaolingwei Street 200, Nanjing 210094, China
[b] Key Laboratory of Nano-Devices and Applications, Suzhou Institute of Nano-Tech and Nano-Bionics, Chinese Academy of Sciences, Ruoshui Road 398, Suzhou 215123, China
[c] Department of Materials Science & Engineering, North Carolina State University, Raleigh, NC 27695, USA

ARTICLE INFO

Article history:
Received 18 February 2016
Received in revised form
31 July 2016
Accepted 22 September 2016
Available online 22 September 2016

Keywords:
Carbon nanotube fiber
Strengthening
Toughening
Cross-link
Strapping

ABSTRACT

Cross-linked carbon nanotube (CNT) networks provide efficient load and charge transfer within their assemblies. Injection chemical vapor deposition (iCVD) has been widely used to obtain such structure with rich cross-links. However, in the iCVD process, a certain organic by-products, probably dioctyl phthalate (DOP) molecules, co-exist in the CNT network, which degrade the interfacial property between CNTs. The removal of the DOP-like molecules can remarkably strengthen the CNT cross-links, improving the assembly's modulus, but it also causes significant loss in toughness. Here we report that strapping up the strengthened cross-links with long-chain and inherently polar polymer polyvinylidene fluoride (PVDF) can result in a simultaneous strengthening and toughening of CNT assemblies, e.g. CNT fibers. This finding represents a new strategy to develop advanced CNT-based macroscopic assembly materials.

1. Introduction

Carbon nanotubes (CNTs) are promising candidates to serve as building blocks for high-performance composite materials. By using an array-based spinning [1–3] or directly collecting CNT aerogels grown with an injection chemical vapor deposition (iCVD) growth [4–6], two types of CNT fibers can be obtained, namely the array-spun and iCVD fibers. These fibers contain highly aligned and entangled (cross-linked) CNTs, respectively. Besides the different assembly styles, there also exist a certain content of catalyst particles and hydrocarbon molecules inside the iCVD fibers. These fibers differ from each other greatly in mechanical and electrical responses. For example, the array-spun fibers have a tensile strength of 1.33–1.58 GPa [7] or 2.32–2.5 GPa [8] after being densified with ethylene glycol or infiltrated with bismaleimide polymers, respectively, while the iCVD fibers possess high plasticity and thus a high toughness due to their large strain at break [5,9,10]. For electrical performances, the iCVD fibers exhibit piezoresistivity under applied high tensile strains and can potentially be used as embedded sensors in composite applications [11]. These results indicate that the high ultimate strain of iCVD fiber has advantage in its future application in wearable electronics, energy devices, health systems, and textile composites.

The introduction of stable CNT cross-links has become an important way to bring CNT application closer to reality [12]. Different from those reported approaches to form cross-links, including irradiation [13], electron or iron beam deposition [14], soldering [15], chemical modifying [16], and doping [17], the iCVD assemblies of CNTs demonstrate many advantages due to the richness of self-assembled CNT cross-links. The aim of this study is to focus on the physics of the cross-links in the iCVD assemblies, especially in the form of fibers. In order not to change the intrinsic mechanical and electrical properties of individual CNTs, non-covalent treatments are investigated, including thermal and electrical (heating) treatments and polymer infiltration.

In the iCVD CNT assemblies, organic compounds were by-products during the growth. Although their mass fraction was

* Corresponding author.
** Corresponding author.
E-mail addresses: xhzhang2009@sinano.ac.cn (X. Zhang), qwli2007@sinano.ac.cn (Q. Li).

http://dx.doi.org/10.1016/j.compscitech.2016.09.019
0266-3538/

small, the organic by-products had remarkable influences in increasing plasticity and reducing tensile strength, owing to their nature as plasticizer, similar to molecule of dioctyl phthalate (DOP, $C_{24}H_{38}O_4$). The removal of the organic molecules by means of thermal and electrical heating enhanced the strength of CNT cross-links by sacrificing plasticity.

In this study, by introducing non-covalent strapping with long-chain molecules, both strengthening and toughening effects were observed for the iCVD fibers. The two major influences of strapping are the improved load transfer between cross-linked CNTs due to the increased interfacial interactions from the molecular straps, and the longer sliding distance between adjacent CNTs. Among different long-chain polymers, polyvinylidene fluoride (PVDF) demonstrated the highest ability to strengthen and toughen the fibers. The highest specific strength and toughness were up to 0.69 N tex^{-1} and 146.7 J g^{-1}. The strapping-up method represents a new strategy to efficiently utilize entangled CNTs, and can be well applied in other forms of CNT assemblies like films and foams [18].

2. Results and discussion

2.1. Organic compounds between CNTs

Different from the array-spun CNT fibers, the CNTs in iCVD fibers are not aligned but heavily entangled with each other to form CNT networks (Fig. 1a). Such entanglement requires additional energy cost to align the CNTs and thus results in high plasticity and toughness. Further, there are also many by-products formed during the injection growth, such as amorphous carbon, iron nanoparticles, and organic compounds like aromatic hydrocarbons. Unfortunately, little attention has been paid to these by-products as their mass fractions are not high. By considering the intimate interaction between CNT and a wide variety of organic molecules, it is suspected that the existence of organic compounds between CNTs can significantly influence the mechanical, electrical, and thermal properties of the iCVD fibers. For simplicity, the iCVD fibers shall be simply called as CNT fibers hereafter.

To find out their possible molecular structure, Fourier transform infrared spectroscopy (FTIR) was performed. The as-produced CNT films were soaked in acetone and stirred for 48 h to dissolve the organic molecules that covered the CNTs (Fig. 1b). By evaporating acetone to concentrate the solution, we obtained a light yellow and oily liquid (Fig. 1c). The FTIR result was compared with that of DOP, see Fig. 1d, which shows the two curves matched with each other in an extremely high level. This indicated that the major compounds of the organic molecules was DOP-like, containing aromatic ring (1580 and 1600 cm^{-1}), carboxylic acid ester (1124/1288 and 1730 cm^{-1} for C–O and C–O stretching), and hydrocarbon chain (2850–3000 cm^{-1} for C–H stretching, 1380 cm^{-1} for methyl group, and 1460 cm^{-1} for methylene group). Though the basic reaction principle was still unknown, we supposed that these DOP-like molecules were formed at the end of the growth process, far away from the reaction zone, where the temperature was pretty low that allowed the existence of organics. The mass fraction of these DOP-like molecules was 7–9 wt%, according to the thermogravimetric (TG) measurement (Fig. 1e).

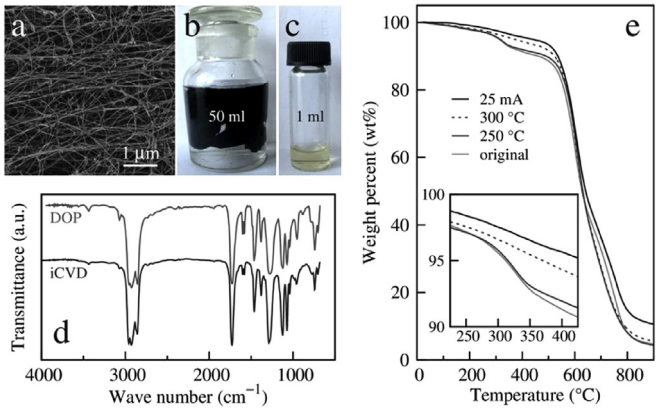

Fig. 1. Characterization of as-produced CNT assemblies. (a) The CNTs were entangled with each other. (b, c) The organic compounds were dissolved with acetone and showed light yellow in the concentrated solution. (d) FTIR spectra of the organic compounds and DOP molecules. (e) TG results for the as-produced, thermo-treated (250 and 300 °C), and electro-treated CNT fibers. (For interpretation of the references to colour in this figure legend, the reader is referred to the web version of this article.)

2.2. Effect of removal of organic compounds

The organic compounds play significant roles in determining the mechanical properties of CNT fibers. The first way to show such influence is to get rid of them by means of thermal or electrical treatments. The specific tensile strength of the as-produced CNT fibers was ~0.17 N tex^{-1}, a unit widely used in the fiber industry, and the strain at break was 9–13%. This reminded us that DOP is widely used as plasticizers and can substantially improve the ductility for most of the synthetic resins and rubbers. Similarly, the existence of DOP-like molecules in CNT assemblies is likely an important source for the high plasticity. By thermally removing the DOP-like molecules at 300 °C, the strength increased up to ~0.27 N tex^{-1} and the strain decreased down to 4.7–7% (Fig. 2a). These changes indicated that the organic compounds acted not only as a surface modifier for plasticity but also a weakening agent to the cross-links between CNTs. After the DOP removal, the cross-links became stronger, which led to lower fracture strain, higher elastic modulus (from ~3.6 to ~6.4 N tex^{-1}), and higher strength.

The electrical treatment led to better improvement on the tensile strength. Using electric currents of 20–30 mA increased the final strength up to 0.33–0.35 N tex^{-1} (Fig. 2a) and the modulus to

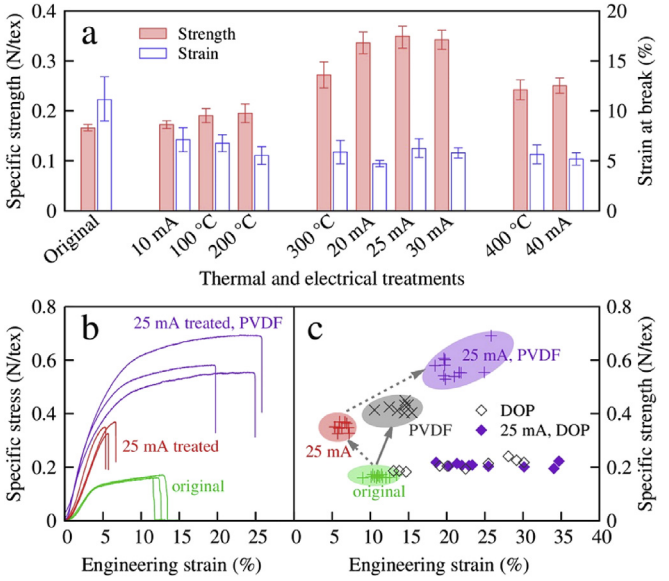

Fig. 2. Strengthening and toughening of CNT fibers. (a) Comparison in fracture strain and specific strength for thermo- and electro-treated CNT fibers. All plots were based on 10–15 tensile tests. (b) Typical stress-strain curves for the as-produced, electro-treated, and PVDF-toughened CNT fibers. (c) PVDF and DOP demonstrated different abilities to strengthen and toughen CNT fibers.

~7.1 N tex^{-1}, see also the typical curves for the 25-mA treatment in Fig. 2b. Interestingly, the Raman G band of CNT fiber shifted from 1585 cm^{-1} (no current) to 1582.6, 1576.5, and 1573.2 cm^{-1}, after the 10-, 20-, and 25-mA treatments, respectively. According to the linear dependence between temperature and G-band shift [19], the temperatures under these currents were about 60, 213, and 317 °C, respectively. This means that although the final temperature was similar, the 25-mA treatment showed significant advantages over the 300-°C thermal treatment; it took just 3–5 min to remove the organics as fully as possible while it required at least 30 min for the thermal treatment. This is because that the electro-heating can take place immediately from the inner part of CNT fibers and allow the full removal of the DOP-like molecules. Another possible reason is the electro-induced densification between CNTs by the electromagnetic force between parallel currents passing through them [8,20].

Notice that we divided the obtained results into four groups in Fig. 2a. The DOP-like molecules could not be completely removed while the temperature was lower than 300 °C. So, the strength of the 100-°C, 200-°C and 10-mA current treated samples just remained or slightly increased. Overheating using a high temperature or current might destroy the sp^2 hybridization and result in the decrease in strength. The optimal treatment parameter was confirmed to be around 300 °C or 25 mA.

2.3. Comparison of PVDF and DOP reintroduction

As the DOP-like molecules benefit plasticity while the removal of them makes the interfacial load transfer more efficient, it suggested that infiltrating some other polymer molecules into the thermo- or electro-treated CNT fibers might increase their plasticity while maintaining the improved tensile strength. PVDF was chosen for its combination of flexibility, low weight, low thermal conductivity, high chemical corrosion resistance, heat resistance, and high mechanical performance. Fig. 2b shows that PVDF not only strengthened the fiber strength and modulus, but also further increased the strain at break. PVDF is a special plastic material in the fluoropolymer family due to its long C–C chain and the large polarity of C–F bond [21]. The polar side groups enhance the intermolecular forces and thus introduce more paths for load transfer at interfaces. This was reflected by their improved modulus of ~8.9 N tex^{-1} as shown in Fig. 2b. In addition, as a long-chain polymer, PVDF wraps around the cross-links between CNTs and thus ductilizes these cross-links by allowing longer sliding distances between CNTs, resulting in the increased toughness. Notice that, the PVDF content after the infiltration (7–9.7 wt%) was very close to the organic content in the original fibers as shown in Fig. 1c. This can be also confirmed by measuring the linear mass density; it changed from 6.83 to 6.24 dtex (1 dtex = 0.1 g km^{-1}) by electrically removing the DOP-like impurities (in agreement with the TG measurement), and increased up to 6.93 dtex after the PVDF infiltration.

It is necessary to compare the above result with that of PVDF enhanced untreated CNT fibers. Fig. 2c shows that the direct introduction of PVDF also led to strengthening and toughening, but the improvements were much smaller due to the existence of DOP-like molecules. This means that the DOP family and PVDF play totally different roles in affecting the mechanical properties of CNT cross-links and they may compete with each other.

DOP was also introduced into the untreated and 25-mA treated fibers, respectively. As shown in Fig. 2c, the increase in strength was small (~0.04 N tex^{-1}), while the strain at break more than doubled. This reflected the nature of plasticizer for DOP. Notice that there was no clear difference whether the electrical treatment was applied before the infiltration, as the DOP content of 17.1–22.7 wt% after the infiltration was much larger than that of the original fibers.

2.4. Strapping-up mechanism

Fig. 3a schematically shows the different cross-link structures affected by DOP and PVDF. DOP is a molecule containing one aromatic ring and two 9-bond chains and its molecular weight is 390.6 g mol^{-1}. Its dimensions have the same order of magnitude with, and even smaller than the CNT's diameter. As a result, DOP molecules can easily move into the inter-tube spaces and act as lubricants rather than bonding the neighboring CNTs. On the contrary, PVDF has a much larger molecular weight (over 2.5×10^3 g mol^{-1}, depending on the number of monomers) and thus a low movability to separate cross-linked CNTs. Moreover, the fluorine prefers to bond next to each other while interact with CNT [22] and the tube-F bond energies are larger for F atoms bonded to adjacent carbon atoms [23]. So, fluorines are more inclined to adds around the tube rather than along the tube [24]. Thus, the long-chain structure facilitates the wrapping around cross-linked CNTs and the high polarity of C–F bond is important to increase the interfacial binding energy.

The scanning electron microscopy (SEM) image at the fiber fracture can clearly show how the CNTs responded to the plastic strain. Long-distance sliding between big CNTs bundles was widely observed for the CNT fiber that contained a certain amount of oily DOP-like substance (Fig. 3b). Due to the easy sliding, there was also

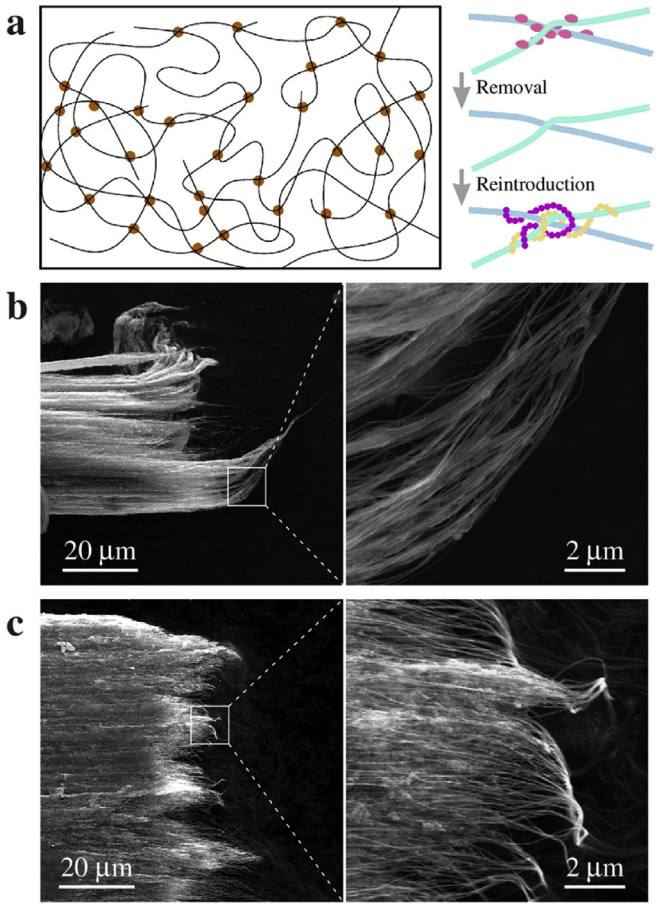

Fig. 3. (a) Schematics of the cross-link structure of the iCVD fiber with DOP bridging two CNTs, electro-treated neat tubes and PVDF-strapped tubes. (b) SEM images of the fracture for a fiber with DOP-like molecules inside. (c) SEM images of the fracture for a current-treated fiber with PVDF reintroduction.

splitting of the fractured end. The fiber bifurcated into several big bundles and the big ones continued to split into numerous smaller bundles. For the CNT/PVDF composite fiber, the integral sliding phenomenon was significantly restrained while the localized sliding between tiny strapped CNT bundles took place and the CNT cross-links were well maintained even at the fracture (Fig. 3c). The fracture was much trimmer, however tiny long strapped bundles were drew out from the fiber and distributed uniformly along the edge of the fracture. Obviously, the DOP-like molecules acted as lubricants and PVDF well strapped up the cross-links.

2.5. Electrical properties

The removal of the DOP-like molecules from the as-produced fiber also affected significantly the fiber's electrical property, as reflected by the change in the linear electrical resistance (the resistance per unit fiber length), see Fig. 4a. During the electro-treatment, the DOP-like molecules evaporated and the linear resistance gradually increased up from 8.04 to 15.37 Ω mm^{-1}. This indicated that the existence of DOP-like molecules allowed more pathways for electron transport.

The reintroduction of DOP and PVDF into electro-treated fibers further increased the linear resistance, up to 16.90 and 18.76 Ω mm^{-1}, respectively. Such result agreed well with their ability to tune the interfaces and cross-links between CNTs, as described above. The DOP permeation caused more insulate contact between the CNTs and the strapping with PVDF also induced high level of surface covering which hindered the electron transportation.

The only surprising phenomenon was that the DOP-like molecules and DOP molecules played totally different roles in modifying the interfacial electronic property. We thus suspect that the DOP-like molecules was electronically conductors. To show this, we simply estimated the conductivity of DOP-like molecules solution. It showed good conductivity (>50 S m^{-1}) although the content of DOP-like molecules in the acetone solvent was not high, while solvent (acetone) and DOP are both nonconductive.

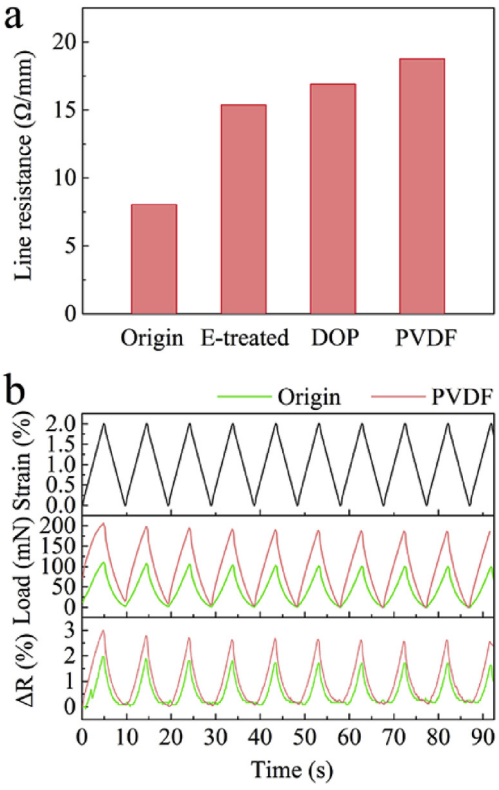

Fig. 4. (a) Line resistance of the same sample: the values of the origin, electro-treated, DOP and PVDF infiltrated fiber were measured orderly. (b) The performance comparison of strain sensors made of the original fiber and the PVDF-enhanced fiber.

The resistance of iCVD fiber was also dependent on the tensile strain upon stretching [25]. As the PVDF-infiltrated fiber exhibited higher elastic modulus (~8.9 N tex^{-1}) and larger elastic region (up to ~7% in strain) than the as-produced fiber (~3.6 N tex^{-1} and <4%, respectively), see Fig. 2c, the new fiber might act as a high efficient strain sensor. To show this, a comparison between the PVDF-infiltrated and as-produced fibers was performed by measuring their resistance upon cyclic stretching between 0 and 2% (Fig. 4b). The PVDF treatment resulted a resistance (as respect to the original value without stretching) variation up to 3%, more detectable than the 2% variation for the as-produced fiber. Besides, due to the strapping mechanism, the load variation during the cyclic stretching was nearly doubled for the PVDF treatment.

3. Conclusion

In this study, we've proved that there are DOP-like molecules formed in the iCVD fibers during their growth process. This organic impurity can be evaporated by high temperature treatment or electrical treatment, and the latter is more effective in improving the fiber strength. The appropriate treat condition is around 300 °C or 20–30 mA, respectively. The strength enhancement is assumed to be caused by better load transfer between CNTs after DOP-like lubricant is removed. This assumption is proved by the reintroduction of DOP, which increased the fiber fracture strain while decreasing the treated fibers' strength. PVDF was found to be able to simultaneously increase the breaking strain and strength, which led to a high toughness of 146.7 J g^{-1}. The reason behind this enhancement may be due to the high polarity of the C–F bond and the peculiarity of fluorine-binding to CNT's sidewalls.

4. Experimental section

The iCVD technique was used to produce CNT fibers [4–6]. For the CNT growth, a mist of ethanol, ferrocene (2 wt%), and thiophene (1 vol%) was injected into a heated gas flow reactor. The diameter of the reactor tube was 80 mm and the injection rate was 20–30 ml h^{-1}. A gas mixture of argon (3500 sccm) and hydrogen (4250 sccm) were also injected into as a carrier gas. The temperature in reaction zone was 1300 °C. The grown CNTs formed a sock-like aerogel in the gas flow and were blown out by the carrier gas. The CNT aerogel was led to pass through a water bath to get densified and become fiber-like, in the similar way that was reported very recently [10]. Finally, a continuous iCVD fiber with a length longer than several meters was collected on a winder. The CNT diameter ranged from 5 to 10 nm and there were many double- and triple-walled CNTs as shown in Fig. 5.

During the growth, some decomposed hydrocarbons deposited from iron particles to form CNTs in high-temperature region while some other reacted with each other to form organic compounds in the pretty cold zone. These compounds finally converted into by-products between the grown CNTs. Thermal or electrical treatments were used to remove them by evaporation. Different heating temperatures were used in air atmosphere, ranging from 100 to 400 °C, and electric currents of 10–40 mA were applied to pass through CNT fibers otherwise. The electro treatment can result in a rapid heating and can further introduce attractive forces between parallel CNTs due to the electromagnetic interactions, as we have reported previously [8].

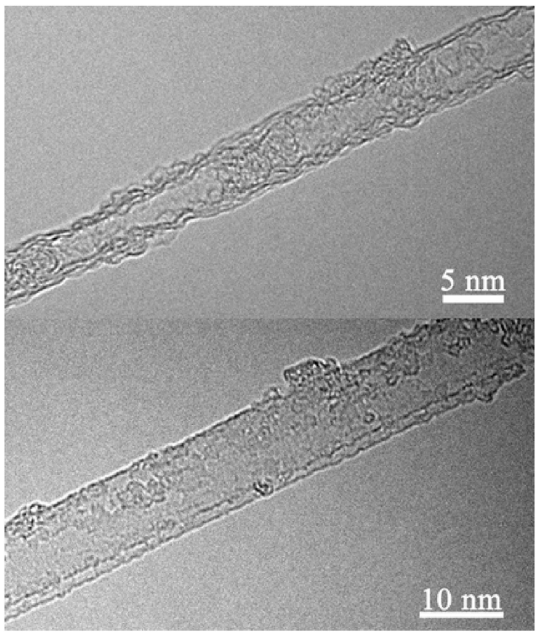

Fig. 5. Two transmission electron microscopy images of the CNTs.

In order to study how the interfaces between CNTs affect the overall mechanical responses, DOP and PVDF were impregnated or reintroduced into the untreated, thermo-, and electro-treated CNT fibers. The CNT fibers were soaked in their dilute solutions (both 0.1 wt%) for 2 h to perform the reintroduction, and the solvent were acetone and dimethyl formamide (DMF), respectively. After the PVDF infiltration, a similar current-drying method was adopted to rapidly remove the solvent. The current was just 10–15 mA as the electro-heating is high enough to evaporate DMF without influence the thermodynamics of PVDF.

Raman spectrometer was used to characterize the defect degree of CNT and the temperature generated by the current in the fiber. Thermogravimetric analyzer was used to identify the quantity of the organics remained in the fiber. The linear density was measured by a fiber fineness meter (XD-1) and was further confirmed by a high-precision analytical balance (XP2U, METTLER TOLEDO). Mechanical tests were performed on a UTM, which has a 500 mN max load sensor and an accuracy of 1 nN, respectively. The samples were all fixed on paper template with a 6 mm gauge length and tested at a stretching rate of 0.001 s^{-1}.

Acknowledgment

The authors thank financial supports from the National Natural Science Foundation of China (21273269, 11302241, 11404371, 21473238), the Youth Innovation Promotion Association, Chinese Academy of Sciences (Grant to X.Z.), and Suzhou Industrial Science and Technology Program (ZXG201416).

References

[1] M. Zhang, K.R. Atkinson, R.H. Baughman, Multifunctional carbon nanotube yarns by downsizing an ancient technology, Science 306 (2004) 1358–1361.
[2] J. Zhao, X. Zhang, J. Di, G. Xu, X. Yang, X. Liu, et al., Double-peak mechanical properties of carbon-nanotube fibers, Small 6 (2010) 2612–2617.
[3] J.J. Jia, J.N. Zhao, G. Xu, J.T. Di, Z.Z. Yong, Y.Y. Tao, et al., A comparison of the mechanical properties of fibers spun from different carbon nanotubes, Carbon 49 (2011) 1333–1339.
[4] Y.L. Li, I.A. Kinloch, A.H. Windle, Direct spinning of carbon nanotube fibers from chemical vapor deposition synthesis, Science 304 (2004) 276–278.
[5] M. Motta, A. Moisala, I.A. Kinloch, A.H. Windle, High performance fibres from 'dog bone' carbon nanotubes, Adv. Mater. 19 (2007) 3721–3726.
[6] K. Stano, K. Koziol, M. Pick, M. Motta, A. Moisala, J. Vilatela, et al., Direct spinning of carbon nanotube fibres from liquid feedstock, Int. J. Mater. Form. 1 (2008) 59–62.
[7] S. Li, X. Zhang, J. Zhao, F. Meng, G. Xu, Z. Yong, et al., Enhancement of carbon nanotube fibres using different solvents and polymers, Compos. Sci. Technol. 72 (2012) 1402–1407.
[8] F. Meng, X. Zhang, R. Li, J. Zhao, X. Xuan, X. Wang, et al., Electro-induced mechanical and thermal responses of carbon nanotube fibers, Adv. Mater. 26 (2014) 2480–2485.
[9] K. Koziol, J. Vilatela, A. Moisala, M. Motta, P. Cunniff, M. Sennett, et al., High-performance carbon nanotube fiber, Science 318 (2007) 1892–1895.
[10] J.N. Wang, X.G. Luo, T. Wu, Y. Chen, High-strength carbon nanotube fibre-like ribbon with high ductility and high electrical conductivity, Nat. Commun. 5 (2014) 3848.
[11] A.S. Wu, T.W. Chou, J.W. Gillespie, D. Lashmore, J. Rioux, Electromechanical response and failure behaviour of aerogel-spun carbon nanotube fibres under tensile loading, J. Mater. Chem. 22 (2012) 6792.
[12] Y. Cui, M. Zhang, Cross-links in carbon nanotube assembly introduced by using polyacrylonitrile as precursor, ACS Appl. Mater. Inter. 5 (2013) 8173–8178.
[13] T. Filleter, H.D. Espinosa, Multi-scale mechanical improvement produced in carbon nanotube fibers by irradiation cross-linking, Carbon 56 (2013) 1–11.
[14] M.S. Wang, L.M. Peng, J.Y. Wang, Q. Chen, Shaping carbon nanotubes and the effects on their electrical and mechanical properties, Adv. Funct. Mater. 16 (2006) 1462–1468.
[15] J.A. Rodríguez-Manzo, M.S. Wang, F. Banhart, Y. Bando, D. Golberg, Multi-branched junctions of carbon nanotubes via cobalt particles, Adv. Mater. 21 (2009) 4477–4482.
[16] Y. Zhang, A.A. Broekhuis, M.C.A. Stuart, T. Fernandez Landaluce, D. Fausti, P. Rudolf, et al., Cross-linking of multiwalled carbon nanotubes with polymeric amines, Macromolecules 41 (2008) 6141–6146.
[17] D.P. Hashim, N.T. Narayanan, J.M. Romo-Herrera, D.A. Cullen, M.G. Hahm, P. Lezzi, et al., Covalently bonded three-dimensional carbon nanotube solids via boron induced nanojunctions, Sci. Rep. 2 (2012) 363.
[18] L. Liu, W. Ma, Z. Zhang, Macroscopic carbon nanotube assemblies: preparation, properties, and potential applications, Small 7 (2011) 1504–1520.
[19] Q.W. Li, C.H. Liu, X.S. Wang, S.S. Fan, Measuring the thermal conductivity of individual carbon nanotubes by the Raman shift method, Nanotechnology 20 (2009) 145702.
[20] W. Guo, C. Liu, F. Zhao, X. Sun, Z. Yang, T. Chen, et al., A novel electromechanical actuation mechanism of a carbon nanotube fiber, Adv. Mater. 24 (2012) 5379–5384.
[21] P. Murray-Rust, W.C. Stallings, C.T. Monti, R.K. Preston, J.P. Glusker, Intermolecular interactions of the carbon-fluorine bond: the crystallographic environment of fluorinated carboxylic acids and related structures, J. Am. Chem. Soc. 105 (1983) 3206–3214.
[22] R.L. Jaffe, Quantum chemistry study of fullerene and carbon nanotube fluorination, J. Phys. Chem. B 107 (2003) 10378–10388.
[23] C.W. Bauschlicher Jr., Hydrogen and fluorine binding to the sidewalls of a (10,0) carbon nanotube, Chem. Phys. Lett. 322 (2000) 237–241.
[24] K.F. Kelly, I.W. Chiang, E.T. Mickelson, R.H. Hauge, J.L. Margrave, X. Wang, et al., Insight into the mechanism of sidewall functionalization of single-walled nanotubes: an STM study, Chem. Phys. Lett. 313 (1999) 445–450.
[25] Q.W. Li, Y. Li, X.F. Zhang, S.B. Chikkannanavar, Y.H. Zhao, A.M. Dangelewicz, et al., Structure-dependent electrical properties of carbon nanotube fibers, Adv. Mater. 19 (2007) 3358–3363.